

Baryonic form factors induced by tensor currents in light-front approach

Hang Liu¹, Wei Wang^{1,2,*} and Zhi-Peng Xing^{3,4,†}

¹*INPAC, Key Laboratory for Particle Astrophysics and Cosmology (MOE), Shanghai Key Laboratory for Particle Physics and Cosmology, School of Physics and Astronomy, Shanghai Jiao Tong University, Shanghai 200240, China*

²*Southern Center for Nuclear-Science Theory (SCNT), Institute of Modern Physics, Chinese Academy of Sciences, Huizhou 516000, Guangdong Province, China*

³*Tsung-Dao Lee Institute, Shanghai Jiao Tong University, Shanghai 200240, China*

⁴*Department of Physics and Institute of Theoretical Physics, Nanjing Normal University, Nanjing, Jiangsu 210023, China*



(Received 6 May 2023; accepted 10 July 2023; published 3 August 2023)

Inspired by the recent anomalies on the lepton flavor universalities, we present an investigation of baryonic form factors induced by heavy-to-light tensor currents. With the light-front quark model, we calculate the tensor form factors, and the momentum distributions are accessed with two parametrization forms. Numerical results for the form factors at $q^2 = 0$ are derived and parameters in q^2 distributions are obtained through extrapolation. Our results are helpful for the analysis of new physics contributions in the heavy-to-light transition.

DOI: [10.1103/PhysRevD.108.035008](https://doi.org/10.1103/PhysRevD.108.035008)

I. INTRODUCTION

Nowadays testing the standard model (SM) of particle physics and hunting for new physics (NP) beyond the SM is a foremost task in particle physics. In recent years, heavy flavor physics has received remarkable attentions and quite interestingly some anomalies are found in weak decays of heavy mesons and baryons. Hints for the lepton flavor universality (LFU) deviating from the standard model were found recently in ratios of branching fractions such as $R(D^{(*)})$ [1–9], $R(J/\psi)$ [10], and $R(\Lambda_c)$ [11]. A collection of the latest experimental measurement is given as [12]

$$\begin{aligned} \mathcal{R}_{\text{exp}}(D) &= 0.441 \pm 0.060 \pm 0.066, \\ \mathcal{R}_{\text{exp}}(D^*) &= 0.247 \pm 0.015 \pm 0.015 \pm 0.012, \\ \mathcal{R}_{\text{exp}}(J/\psi) &= 0.71 \pm 0.17 \pm 0.18, \\ \mathcal{R}_{\text{exp}}(\Lambda_c) &= 0.242 \pm 0.026 \pm 0.040 \pm 0.059, \end{aligned} \quad (1)$$

while the recent average of SM predictions on $R(D^{(*)})$ is given as [12]

$$\begin{aligned} \mathcal{R}_{\text{SM}}(D) &= 0.298 \pm 0.004, \\ \mathcal{R}_{\text{SM}}(D^*) &= 0.254 \pm 0.005. \end{aligned} \quad (2)$$

One can see that the latest experimental measurement on $R(D^{(*)})$ shows about a 2σ standard deviation from SM prediction. While the most precise SM predictions on $R(J/\psi)$ and $R(\Lambda_c)$ are generally consistent with experimental measurements [13–15],

$$\begin{aligned} \mathcal{R}_{\text{SM}}(J/\psi) &= 0.258 \pm 0.004, \\ \mathcal{R}_{\text{SM}}(\Lambda_c) &= 0.324 \pm 0.004, \end{aligned} \quad (3)$$

there are also noticeable discrepancies in the central values between the SM predictions and experimental results. Thereby, more theoretical and experimental investigations are needed to clarify this obscure situation.

Many interesting theoretical explanations have emerged to explain these deviations, including contributions from new physics. For a recent review on the topic, please refer to Ref. [16]. In some of these analyses, new effective NP Hamiltonians have been introduced [17–26]. Unlike the SM, some of these Hamiltonians introduce a new structure of $b \rightarrow c$ current in the hadron matrix element: the tensor current. While the tensor current contribution resolves the current discrepancies, it should be noticed that this contribution can also affect baryonic decay processes induced by the $b \rightarrow c\ell\nu$. Though the explicit contributions of the tensor current depend on the details of NP models, the low-energy nonperturbative matrix elements, namely form factors, are universal and mandatory. Therefore for a

*wei.wang@sjtu.edu.cn

†Corresponding author: zpxing@sjtu.edu.cn

Published by the American Physical Society under the terms of the [Creative Commons Attribution 4.0 International license](https://creativecommons.org/licenses/by/4.0/). Further distribution of this work must maintain attribution to the author(s) and the published article's title, journal citation, and DOI. Funded by SCOAP³.

comprehensive NP model-independent analysis, the results on baryonic tensor form factors are called for.

In this work, we aim to present an exploration of these new form factors, and in the calculation employ the light-front quark model (LFQM) [27–32]. The baryon system can be treated in a similar manner with a meson under the quark-diquark assumption [33–35]. It is noteworthy that a three-quark vertex function has been explored in LFQM, and the investigations in Refs. [36] and [37] have shown consistent results with the two approaches using a three-quark and diquark vertex. This also validates the diquark approach that will be adopted in this work.

The rest of this paper is arranged as follows. We give the definition of tensor form factors and the theoretical framework of LFQM in Sec. II. The tensor form factors are explicitly calculated in Sec. III, and the analytical expressions are given. Numerical analysis and discussions are given in Sec. IV. In the end, we give a brief summary.

II. THEORETICAL FRAMEWORK

To account for the anomalies in heavy quark physics, NP contributions are typically needed. In a general analysis, the Hamiltonian after integrating out the degree of freedoms over the m_b scale can be expressed as

$$\mathcal{H}_{\text{eff}} \sim \sum_{\Gamma, \Gamma'} C_{\Gamma, \Gamma'} \times [\bar{c}\Gamma b][\bar{l}\Gamma' \nu], \quad (4)$$

where the $C_{\Gamma, \Gamma'}$ are the Wilson coefficients and the $\Gamma^{(i)}$ denote all the possible Lorentz structures $\{1, \gamma^\mu, \gamma_5, \gamma^\mu \gamma_5, \sigma^{\mu\nu}\}$. The tensor current does not exist in the SM, and as a result the corresponding form factors are not well understood in previous theoretical analyses [21,22,24,38,39].

This work will focus on the antitriplet b -baryon to antitriplet c -baryon and sextet b -baryon to sextet c -baryon processes:

$$\begin{aligned} \bar{3} \rightarrow \bar{3}: \Lambda_b^0 \rightarrow \Lambda_c^+, \quad \Xi_b^0 \rightarrow \Xi_c^+, \quad \Xi_b^- \rightarrow \Xi_c^0 \\ 6 \rightarrow 6: \Sigma_b^+ \rightarrow \Sigma_c^{++}, \quad \Sigma_b^- \rightarrow \Sigma_c^0, \quad \Sigma_b^0 \rightarrow \Sigma_c^+, \\ \Xi_b^{0'} \rightarrow \Xi_c^{+'}, \quad \Xi_b^{-'} \rightarrow \Xi_c^{0'}, \quad \Omega_b^- \rightarrow \Omega_c^0. \end{aligned} \quad (5)$$

Inserting the Dirac Gamma matrices in a bilinear local quark current sandwiched between the b -baryons and c -baryons, one can define the pertinent form factors:

$$\begin{aligned} \langle \mathcal{B}'(P', S') | \bar{c} i \sigma^{\mu\nu} b | \mathcal{B}(P, S) \rangle \\ = \bar{u}(P', S') \left[f_1(q^2) i \sigma^{\mu\nu} + \Sigma_{\sigma\rho}^{\mu\nu} \left(\frac{f_2(q^2)}{M} \gamma^\sigma P^\rho \right. \right. \\ \left. \left. + \frac{f_3(q^2)}{M'} \gamma^\sigma P'^\rho + \frac{f_4(q^2)}{MM'} P^\sigma P'^\rho \right) \right] u(P, S), \end{aligned} \quad (6)$$

where Dirac operator $\sigma^{\mu\nu} = \frac{i}{2}(\gamma^\mu \gamma^\nu - \gamma^\nu \gamma^\mu)$ and $\Sigma_{\sigma\rho}^{\mu\nu} = g_\sigma^\mu g_\rho^\nu - g_\sigma^\nu g_\rho^\mu$. The form factors in the $\langle \mathcal{B}'(P', S') | \bar{c} \sigma^{\mu\nu} \gamma_5 b | \mathcal{B}(P, S) \rangle$

matrix element can be straightforwardly obtained from Eq. (6) by making use of $\sigma^{\mu\nu} \gamma_5 = -\frac{i}{2} \epsilon^{\mu\nu\lambda\rho} \sigma_{\lambda\rho}$.

The form factors defined in a hadronic matrix element are nonperturbative. To evaluate the form factors a relativistic quark model, namely light-front quark model, will be employed. In this framework, it is convenient to use the light-front frame:

$$\begin{aligned} p^\mu &= (p^+, p^-, p_\perp), & p^+ &= p^0 + p^3, \\ p^- &= p^0 - p^3, & p_\perp &= (p^1, p^2). \end{aligned} \quad (7)$$

With the help of the diquark picture, the baryon state containing three quarks can be treated as a meson state which is widely studied in the LFQM [40]. In this picture, the two spectator quarks played a similar role with an antiquark.

For the $J^P = 1/2^+$ baryon state, its wave function is

$$\begin{aligned} |\mathcal{B}(P, S, S_z)\rangle \\ = \int \{d^3 p_1\} \{d^3 p_2\} 2(2\pi)^3 \delta^3(\tilde{P} - \tilde{p}_1 - \tilde{p}_2) \\ \times \sum_{\lambda_1, \lambda_2} \Psi^{SS_z}(\tilde{p}_1, \tilde{p}_2, \lambda_1, \lambda_2) |Q(p_1, \lambda_1)(\text{di})(p_2, \lambda_2)\rangle, \end{aligned} \quad (8)$$

where Q donates the heavy quark which is b/c in our work and “(di)” presents the diquark. The λ_1 and λ_2 are the helicity of quark and diquark respectively. The momentum of them are p_1 and p_2 and the P is the baryon momentum. Both of them are on their mass shell. However, since the baryon states are constructed by a quark and diquark, their momenta cannot be on-shell simultaneously. Thus in the wave function of LFQM the three momentum $\{\tilde{P}, \tilde{p}_1, \tilde{p}_2\}$ are used. They are defined as $\tilde{p} = (p^+, p_\perp)$. The distribution function Ψ in Eq. (8) is

$$\begin{aligned} \Psi^{SS_z}(\tilde{p}_1, \tilde{p}_2, \lambda_1, \lambda_2) &= \frac{1}{\sqrt{2(p_1 \cdot \tilde{P} + m_1 M_0)}} \\ &\times \bar{u}(p_1, \lambda_1) \Gamma_{S(A)} u(\tilde{P}, S_z) \phi(x, k_\perp). \end{aligned} \quad (9)$$

Here Γ is the coupling vertex which embodies the spin of the diquark. For the spin-0 scalar diquark the vertex is Γ_S and for the spin-1 axis-vector diquark the vertex becomes Γ_A . The coupling vertices are shown as

$$\begin{aligned} \Gamma_S &= 1, \\ \Gamma_A &= \frac{\gamma_5}{\sqrt{3}} \left(\not{\epsilon}^* - \frac{M_0 + m_1 + m_2}{\tilde{P} \cdot p_2 + m_2 M_0} \epsilon^* \cdot \tilde{P} \right), \end{aligned} \quad (10)$$

where the \tilde{P} is the sum of on-shell momenta p_1 and p_2 . Though the momentum \tilde{P} is not onshell, one can still define an effective mass as $M_0^2 = \tilde{P}^2$ where $M^2 \neq M_0^2$.

TABLE I. Masses of charm and bottom baryons and input parameters in the momentum distribution wave functions [40].

Baryons	Λ_b^0	Σ_b^+	Σ_b^-	Σ_b^0	Ξ_b^0	Ξ_b^-
Mass(GeV)	5.620	5.811	5.816	5.814	5.792	5.797
Baryons	$\Xi_b^{\prime 0}$	$\Xi_b^{\prime -}$	Ω_b^-	Λ_c^+	Σ_c^{++}	Σ_c^0
Mass(GeV)	5.935	5.935	6.045	2.286	2.454	2.454
Baryons	Σ_c^+	Ξ_c^+	Ξ_c^0	$\Xi_c^{\prime +}$	$\Xi_c^{\prime 0}$	Ω_c^0
Mass(GeV)	2.453	2.468	2.470	2.578	2.579	2.695
Shape parameter(GeV)	$\beta_{c[uq]} = 0.470$		$\beta_{c[sq]} = 0.535$			
	$\beta_{b[uq]} = 0.562$		$\beta_{b[sq]} = 0.623$			

The $\phi(x, k_\perp)$ in Eq. (9) is a Gaussian-type momentum distribution function which is constructed as

$$\phi(x, k_\perp) = 4 \left(\frac{\pi}{\beta^2} \right)^{3/4} \sqrt{\frac{e_1 e_2}{x_1 x_2 M_0}} \exp\left(\frac{-\vec{k}^2}{2\beta^2} \right), \quad (11)$$

where e_1 and e_2 represent the energy of heavy quark Q and diquark in the rest frame of \bar{P} . The β is a phenomenological parameter which is shown in Table I. In Ref. [41], a Gaussian expansion method with a semi-relativistic potential model is applied to determine the momentum distribution wave function and in Ref. [42], the parameters β are extracted by the pole residue. In this work the parameters β are used from Ref. [40].

The x_1 and x_2 in Eq. (11) are the light-front momentum fractions which satisfy the requirements $0 < x_2 < 1$ and $x_1 + x_2 = 1$. The k is the internal momentum which represents the interaction between quark and diquark. So the k and the quark and diquark momenta are

$$\begin{aligned} k_i &= (k_i^-, k_i^+, k_{i\perp}) = (e_i - k_{iz}, e_i + k_{iz}, k_{i\perp}) \\ &= \left(\frac{m_i^2 + k_{i\perp}^2}{x_i M_0}, x_i M_0, k_{i\perp} \right), \end{aligned}$$

$$\begin{aligned} p_1^+ &= x_1 \bar{P}^+, & p_2^+ &= x_2 \bar{P}^+, & p_{1\perp} &= x_1 \bar{P}_\perp + k_{1\perp}, \\ p_{2\perp} &= x_2 \bar{P}_\perp + k_{2\perp}, & k_\perp &= -k_{1\perp} = k_{2\perp}. \end{aligned} \quad (12)$$

With the help of the internal momentum k , the invariant mass square M_0^2 is expressed as

$$M_0^2 = \frac{k_{1\perp}^2 + m_1^2}{x_1} + \frac{k_{2\perp}^2 + m_2^2}{x_2}. \quad (13)$$

The expression of e_i and k_z can also be presented in terms of the internal variables $(x_i, k_{i\perp})$ as

$$\begin{aligned} e_i &= \frac{x_i M_0}{2} + \frac{m_i^2 + k_{i\perp}^2}{2x_i M_0} = \sqrt{m_i^2 + k_{i\perp}^2 + k_{iz}^2}, \\ k_{iz} &= \frac{x_i M_0}{2} - \frac{m_i^2 + k_{i\perp}^2}{2x_i M_0}. \end{aligned} \quad (14)$$

In the following, we use the notation $x = x_2$ and $x_1 = 1 - x$.

III. FORM FACTORS

The hadronic matrix element in Eq. (6) can be expressed by the LFQM as

$$\begin{aligned} &\left\langle \mathcal{B}_c \left(P', \frac{1}{2}, S'_z \right) | \bar{c} i \sigma^{\mu\nu} b | \mathcal{B}_b \left(P, \frac{1}{2}, S_z \right) \right\rangle \\ &= \int \{d^3 p_2\} \frac{\phi'(x', k'_\perp) \phi(x, k_\perp)}{2\sqrt{p_1^+ p_1'^+} (p_1 \cdot \bar{P} + m_1 M_0) (p_1' \cdot \bar{P}' + m_1' M_0')} \\ &\quad \times \sum_{\lambda_2} \bar{u}(\bar{P}', S'_z) [\bar{\Gamma}'(\not{p}' + m_c) i \sigma^{\mu\nu} (\not{p}' + m_b) \Gamma] u(\bar{P}, S_z), \end{aligned} \quad (15)$$

with

$$\bar{P}' = p_1' + p_2, \quad M_0^2 = \bar{P}^2, \quad M_0'^2 = \bar{P}'^2. \quad (16)$$

Since the matrix element can be expressed both at the quark and hadron levels respectively, the form factors can be extracted by solving four equations which are constructed by multiplying the different tensor $\bar{u}(P, S) \{\Gamma_i\}_{\mu\nu} u(P', S')$ to the matrix element in the light-front approach. The Lorentz structure in these tensor is

$$\{\Gamma_i\}_{\mu\nu} = \{\gamma_\mu P'_\nu, \gamma_\mu P_\nu, P_\mu P'_\nu, \gamma_\mu \gamma_\nu\}. \quad (17)$$

Then these form factors are calculated as

$$\begin{aligned} f_1 &= \frac{1}{4Q_+ Q_-} [4MH_1 - 4M'H_2 - 4H_3 + H_4 Q_-], \\ f_2 &= -\frac{1}{2Q_-^2 Q_+} [M(Q_+ + 2MM')H_1 \\ &\quad - 6MM'^2 H_2 - 6MM'H_3 + MM'H_4 Q_-], \\ f_3 &= \frac{1}{2Q_-^2 Q_+} [6M^2 M'H_1 - M'(Q_+ + 2MM')H_2 \\ &\quad - 6MM'H_3 + MM'H_4 Q_-], \\ f_4 &= -\frac{1}{2Q_-^2 Q_+} [6M^2 M'H_1 Q_+ - 6MM'^2 H_2 Q_+ \\ &\quad - 24M^2 M'H_3 + MM'H_4 Q_- Q_+], \end{aligned} \quad (18)$$

where $Q_\pm = (M \pm M')^2 - q^2$ and the function H_i is defined as

$$\begin{aligned}
H_i = & \int \frac{dx d^2 k_\perp}{2(2\pi)^3} \phi'(x', k'_\perp) \phi(x, k_\perp) \times \text{Tr}[(\bar{P}' + M'_0) \Gamma'_{S(A)}] \\
& \times (\not{p}'_1 + m_c) i \sigma_{\mu\nu} (\not{p}_1 + m_b) \Gamma_{S(A)} (\bar{P} + M_0) \{\Gamma_i\}_{\mu\nu} \\
& \times \left(2\sqrt{x'_1 x_1 (p'_1 \cdot \bar{P}' + m'_1 M'_0) (p_1 \cdot \bar{P} + m_1 M_0)} \right)^{-1}.
\end{aligned} \tag{19}$$

In our analysis of the diquark picture, the diquark made of two quarks can be a scalar or an axial vector. Thus the physical form factors estimated by the LFQM should be expressed as the combination of the form factors with scalar and axis vector diquark:

$$F^{[phy]} = c_S \times F_S + c_A \times F_A. \tag{20}$$

The coefficients c_S and c_A can be extracted in the flavor-spin wave function of initial and final baryon states.

Using the scalar and axial-vector diquark wave function [43], $[q, q']_A = (qq' + q'q)/\sqrt{2}$, $[q, q']_S = (qq' - q'q)/\sqrt{2}$, one can write the flavor-spin wave function of the baryon. Since the baryons $\{\Lambda_b^0, \Xi_b^0, \Xi_b^-\}$ and $\{\Lambda_c^+, \Xi_c^+, \Xi_c^0\}$ are the antitriplet in $SU(3)$ flavor symmetry, their flavor-spin wave function is

$$\begin{aligned}
\left| \mathcal{B}_{Qq'q}, S_z = \frac{1}{2} \right\rangle &= \frac{1}{\sqrt{2}} (qq' - q'q) \mathcal{Q} \times \left(\frac{1}{\sqrt{2}} (\uparrow\downarrow\uparrow - \downarrow\uparrow\uparrow) \right) \\
&\equiv [q, q']_S \mathcal{Q}.
\end{aligned} \tag{21}$$

For the sextet baryons, their flavor-spin wave function can be written as

$$\begin{aligned}
\left| \mathcal{B}_{Qq'q}, S_z = \frac{1}{2} \right\rangle &= \frac{1}{\sqrt{2}} (qq' + q'q) \mathcal{Q} \\
&\times \left(\frac{1}{\sqrt{6}} (\uparrow\downarrow\uparrow + \downarrow\uparrow\uparrow - 2\uparrow\uparrow\downarrow) \right) \\
&\equiv -[q, q']_A \mathcal{Q}, \\
\left| \mathcal{B}_{Qqq}, S_z = \frac{1}{2} \right\rangle &= qq\mathcal{Q} \times \left(\frac{1}{\sqrt{6}} (\uparrow\downarrow\uparrow + \downarrow\uparrow\uparrow - 2\uparrow\uparrow\downarrow) \right) \\
&\equiv -[q, q]_A \mathcal{Q},
\end{aligned} \tag{22}$$

where $q, q' = u, d, s$ and $Q = b, c$. For a scalar diquark, namely the baryon triplet, $c_S = 1$ and $c_A = 0$. For the sextet baryons with an axial-vector diquark, $c_S = 0$ and $c_A = 1$. It is worth noting that several studies have suggested that the flavor eigenstates Ξ_c and Ξ'_c may mix with each other to generate the mass eigenstates [44–49]. But the recent lattice QCD indicates a very small mixing angle [50] which is consistent with previous lattice QCD simulation [51]. As a consequence the mixing effect is not taken into account in our analysis.

IV. NUMERICAL ANALYSIS

A. Form factors

Numerical results of tensor form factors will be given in this section. In our calculation, the masses and other parameters of these baryons are shown in Table I.

For the calculation, we use the constituent quark masses from Refs. [52–54]:

$$\begin{aligned}
m_u = m_d = 0.25 \text{ GeV}, \quad m_s = 0.37 \text{ GeV}, \\
m_c = 1.4 \text{ GeV}, \quad m_b = 4.8 \text{ GeV}.
\end{aligned} \tag{23}$$

The masses of the diquarks can be approximated as

$$m_{[qq']} = m_q + m_{q'}, \quad q/q' = u, d, s. \tag{24}$$

For extrapolating the form factors to the full q^2 region, we use the Bourrely-Caprini-Lellouch (BCL) parametrization [55–58] in which the form factors are expanded in powers of a conformal mapping variable. The BCL parametrization is shown as

$$\begin{aligned}
f(t) &= \frac{1}{1 - t/m_R^2} \sum_{k=0}^{k_{\max}} a_k z^k(t, t_0), \\
z(t, t_0) &= \frac{\sqrt{t_+ - t} - \sqrt{t_+ - t_0}}{\sqrt{t_+ - t} + \sqrt{t_+ - t_0}}, \\
t_0 &= t_+ \left(1 - \sqrt{1 - \frac{t_-}{t_+}} \right), \\
t_\pm &= (m_{B_b} \pm m_{B_c})^2.
\end{aligned} \tag{25}$$

The m_R are the masses of the low-lying B_c resonance. Additionally, the q^2 dependence of form factors can also be described by the pole model,

$$F(q^2) = \frac{F(0)}{1 - \frac{q^2}{m_{\text{fit}}^2} + \delta \left(\frac{q^2}{m_{\text{fit}}^2} \right)^2}, \tag{26}$$

where $F(0)$ is the numerical results of form factor at $q^2 = 0$. Using this formula, one can fit the two parameters m_{fit} and δ by the numerical results of form factors with different q^2 . When the fitting results of m_{fit} are imaginary results, we need to modify the parametrization scheme as

$$F(q^2) = \frac{F(0)}{1 + \frac{q^2}{m_{\text{fit}}^2} + \delta \left(\frac{q^2}{m_{\text{fit}}^2} \right)^2}. \tag{27}$$

In this work, we analyze the q^2 dependence of the form factors using both models in Eqs. (25)–(27), respectively. Our strategy is to calculate the form factors at

TABLE II. Numerical results for the tensor form factors of b -baryon to c -baryon transitions induced by $b \rightarrow c$ decays are presented. Results for the parameters δ and m_{fit} are obtained by fitting the form factors with the pole model as in Eq. (26), and the * indicates that m_{fit} is fitted using Eq. (27). The a_0 and a_1 are the parameters in the BCL model in Eq. (25). For the form factors with $q^2 = 0$, i.e., $F(0)$, we estimated their uncertainties caused by the parameters in LFQM, namely, $\beta_{b[qq]}$, $\beta_{c[qq]}$, and m_{di} , which are varied by 10%.

Channel	Form factor	Pole model			BCL model	
		F(0)	δ	m_{fit}	a_0	a_1
$\Lambda_b^0 \rightarrow \Lambda_c^+$	f_1	$0.649 \pm 0.019 \pm 0.079 \pm 0.014$	1.30	6.15	0.66	-0.37
	f_2	$-0.167 \pm 0.039 \pm 0.159 \pm 0.071$	5.12	4.07*	-0.10	-2.61
	f_3	$0.105 \pm 0.024 \pm 0.149 \pm 0.072$	2.80	3.17*	0.05	2.47
	f_4	$-0.042 \pm 0.037 \pm 0.144 \pm 0.065$	0.92	1.79*	0.03	-3.01
$\Sigma_b^+ \rightarrow \Sigma_c^{++}$	f_1	$-0.196 \pm 0.006 \pm 0.019 \pm 0.005$	0.78	5.68	-0.20	0.34
	f_2	$0.057 \pm 0.046 \pm 0.037 \pm 0.010$	2105	21.96*	0.05	0.22
	f_3	$-0.056 \pm 0.039 \pm 0.032 \pm 0.012$	16.19	6.83	-0.06	0.10
	f_4	$0.401 \pm 0.027 \pm 0.047 \pm 0.009$	0.80	4.49	0.46	-2.78
$\Sigma_b^- \rightarrow \Sigma_c^0$	f_1	$-0.197 \pm 0.006 \pm 0.019 \pm 0.005$	0.72	5.63	-0.21	0.37
	f_2	$0.062 \pm 0.046 \pm 0.037 \pm 0.010$	38.34	8.57	0.06	0.02
	f_3	$-0.061 \pm 0.039 \pm 0.032 \pm 0.012$	4.77	5.30	-0.07	0.30
	f_4	$0.404 \pm 0.027 \pm 0.047 \pm 0.009$	0.71	4.43	0.47	-2.94
$\Sigma_b^0 \rightarrow \Sigma_c^+$	f_1	$-0.197 \pm 0.006 \pm 0.019 \pm 0.005$	0.73	5.64	-0.20	0.37
	f_2	$0.060 \pm 0.046 \pm 0.037 \pm 0.010$	73.49	9.94	0.06	0.07
	f_3	$-0.060 \pm 0.039 \pm 0.032 \pm 0.012$	6.01	5.55	-0.07	0.25
	f_4	$0.404 \pm 0.027 \pm 0.047 \pm 0.009$	0.73	4.44	0.47	-2.90
$\Xi_b^0 \rightarrow \Xi_c^+$	f_1	$0.651 \pm 0.022 \pm 0.085 \pm 0.021$	1.80	6.44	0.65	-0.04
	f_2	$-0.214 \pm 0.050 \pm 0.195 \pm 0.100$	4.86	3.99*	-0.13	-3.76
	f_3	$0.140 \pm 0.031 \pm 0.184 \pm 0.102$	2.91	3.21*	0.06	3.49
	f_4	$-0.069 \pm 0.048 \pm 0.179 \pm 0.093$	1.14	2.03*	0.02	-4.12
$\Xi_b^- \rightarrow \Xi_c^0$	f_1	$0.650 \pm 0.022 \pm 0.084 \pm 0.021$	1.73	6.41	0.65	-0.07
	f_2	$-0.214 \pm 0.049 \pm 0.195 \pm 0.100$	5.21	4.10*	-0.14	-3.63
	f_3	$0.141 \pm 0.031 \pm 0.183 \pm 0.102$	3.10	3.30*	0.07	3.35
	f_4	$-0.070 \pm 0.048 \pm 0.179 \pm 0.093$	1.20	2.08*	0.02	-3.97
$\Xi_b'^0 \rightarrow \Xi_c'^+$	f_1	$-0.203 \pm 0.006 \pm 0.021 \pm 0.005$	0.88	5.68	-0.21	0.38
	f_2	$0.070 \pm 0.058 \pm 0.046 \pm 0.012$	171.79	11.97	0.07	0.12
	f_3	$-0.066 \pm 0.049 \pm 0.040 \pm 0.015$	7.33	5.63	-0.07	-0.31
	f_4	$0.434 \pm 0.035 \pm 0.056 \pm 0.010$	0.86	4.52	0.50	-3.13
$\Xi_b'^- \rightarrow \Xi_c'^0$	f_1	$-0.202 \pm 0.006 \pm 0.021 \pm 0.005$	0.89	5.69	-0.21	-0.38
	f_2	$0.069 \pm 0.058 \pm 0.046 \pm 0.012$	407.74	14.72	0.07	0.16
	f_3	$-0.065 \pm 0.049 \pm 0.040 \pm 0.016$	8.76	5.84	-0.07	0.27
	f_4	$0.433 \pm 0.035 \pm 0.056 \pm 0.010$	0.87	4.53	0.50	-3.10
$\Omega_b^- \rightarrow \Omega_c^0$	f_1	$-0.190 \pm 0.005 \pm 0.021 \pm 0.006$	0.78	5.27	-0.203	0.67
	f_2	$0.074 \pm 0.061 \pm 0.048 \pm 0.015$	19.08	7.05	0.077	-0.13
	f_3	$-0.066 \pm 0.052 \pm 0.042 \pm 0.019$	4.19	4.87	-0.076	0.521
	f_4	$0.427 \pm 0.035 \pm 0.061 \pm 0.015$	0.78	4.30	0.504	-3.88

$q^2 = \{0, -0.1, -0.5, -0.7, -1, -1.5\} \text{ GeV}^2$ and fit the parameters in Eqs. (25)–(27). Then we extend the form factors to the physical region with the fitted parameters in these two models. Table II shows the form factors with $q^2 = 0$ and the corresponding fit parameters.

Except the tensor form factor, the form factors defined by the vector and axial-vector current are also calculated for completeness, which are defined as

$$\begin{aligned}
& \langle \mathcal{B}'(P', S') | \bar{c} \gamma^\mu (1 - \gamma_5) b | \mathcal{B}(P, S) \rangle \\
&= \bar{u}(P', S') \left[F_1(q^2) \gamma^\mu + F_2(q^2) \frac{i \sigma^{\mu\nu} q_\nu}{M_B} + F_3(q^2) \frac{q^\mu}{M_B} \right. \\
&\quad \left. - \left(G_1(q^2) \gamma^\mu + G_2(q^2) \frac{i \sigma^{\mu\nu} q_\nu}{M_B} + G_3(q^2) \frac{q^\mu}{M_B} \right) \gamma_5 \right] u(P, S).
\end{aligned} \tag{28}$$

TABLE III. Numerical results for the SM form factors of b -baryon to c -baryon transitions induced by $b \rightarrow c$ decays are presented. The parameters δ and m_{fit} are the results of fitting the pole model in Eq. (26), and the * indicates that m_{fit} is fitted using Eq. (27). For the form factors with $q^2 = 0$, i.e., $F(0)$, we estimated their uncertainties caused by the parameters in LFQM, namely, $\beta_{b[qq]}$, $\beta_{c[qq]}$, and m_{di} , which are varied by 10%.

Channel	Form factor	Pole model parameter			Form factor	Pole model parameter		
		F(0)	δ	m_{fit}		F(0)	δ	m_{fit}
$\Lambda_b^0 \rightarrow \Lambda_c^+$	F_1	$0.637 \pm 0.026 \pm 0.036 \pm 0.008$	0.72	5.50	G_1	$0.625 \pm 0.027 \pm 0.022 \pm 0.014$	0.05	5.13
	F_2	$-0.134 \pm 0.015 \pm 0.001 \pm 0.000$	0.26	3.35	G_2	$0.005 \pm 0.010 \pm 0.040 \pm 0.017$	0.48	1.18*
	F_3	$0.026 \pm 0.015 \pm 0.010 \pm 0.008$	0.51	2.27	G_3	$-0.112 \pm 0.050 \pm 0.118 \pm 0.040$	2.53	3.22*
$\Sigma_b^+ \rightarrow \Sigma_c^{++}$	F_1	$0.549 \pm 0.020 \pm 0.029 \pm 0.003$	0.40	4.00	G_1	$-0.197 \pm 0.009 \pm 0.007 \pm 0.005$	0.07	4.60
	F_2	$0.551 \pm 0.011 \pm 0.021 \pm 0.010$	0.32	4.06	G_2	$0.040 \pm 0.006 \pm 0.010 \pm 0.009$	0.11	2.86
	F_3	$-0.269 \pm 0.007 \pm 0.005 \pm 0.011$	0.31	3.99	G_3	$-0.060 \pm 0.023 \pm 0.032 \pm 0.022$	0.37	2.27
$\Sigma_b^- \rightarrow \Sigma_c^0$	F_1	$0.548 \pm 0.017 \pm 0.026 \pm 0.006$	0.41	4.00	G_1	$-0.196 \pm 0.006 \pm 0.004 \pm 0.009$	0.09	4.63
	F_2	$0.550 \pm 0.006 \pm 0.014 \pm 0.018$	0.32	4.06	G_2	$0.038 \pm 0.006 \pm 0.018 \pm 0.018$	0.10	2.90
	F_3	$-0.268 \pm 0.014 \pm 0.010 \pm 0.020$	0.31	4.00	G_3	$-0.057 \pm 0.023 \pm 0.051 \pm 0.043$	0.37	2.28
$\Sigma_b^0 \rightarrow \Sigma_c^+$	F_1	$0.548 \pm 0.020 \pm 0.029 \pm 0.003$	0.41	4.00	G_1	$-0.196 \pm 0.008 \pm 0.007 \pm 0.004$	0.09	4.63
	F_2	$0.551 \pm 0.012 \pm 0.022 \pm 0.011$	0.32	4.06	G_2	$0.039 \pm 0.006 \pm 0.011 \pm 0.009$	0.10	2.90
	F_3	$-0.268 \pm 0.007 \pm 0.005 \pm 0.011$	0.31	4.00	G_3	$-0.057 \pm 0.023 \pm 0.032 \pm 0.023$	0.37	2.28
$\Xi_b^0 \rightarrow \Xi_c^+$	F_1	$0.635 \pm 0.030 \pm 0.036 \pm 0.006$	0.75	5.56	G_1	$0.620 \pm 0.031 \pm 0.020 \pm 0.014$	0.03	5.23
	F_2	$-0.155 \pm 0.019 \pm 0.001 \pm 0.001$	0.27	3.45	G_2	$0.012 \pm 0.011 \pm 0.046 \pm 0.021$	0.09	2.10*
	F_3	$0.028 \pm 0.017 \pm 0.13 \pm 0.011$	0.49	2.40	G_3	$-0.154 \pm 0.061 \pm 0.141 \pm 0.054$	4.56	4.05*
$\Xi_b^- \rightarrow \Xi_c^0$	F_1	$0.633 \pm 0.030 \pm 0.036 \pm 0.006$	0.74	5.55	G_1	$0.618 \pm 0.031 \pm 0.020 \pm 0.014$	0.01	5.21
	F_2	$-0.154 \pm 0.019 \pm 0.001 \pm 0.001$	0.27	3.45	G_2	$0.013 \pm 0.011 \pm 0.046 \pm 0.021$	0.96	1.86*
	F_3	$0.028 \pm 0.017 \pm 0.013 \pm 0.011$	0.50	2.29	G_3	$-0.157 \pm 0.061 \pm 0.141 \pm 0.054$	3.84	3.79
$\Xi_b'^0 \rightarrow \Xi_c'^+$	F_1	$0.565 \pm 0.019 \pm 0.023 \pm 0.001$	0.44	4.11	G_1	$-0.197 \pm 0.010 \pm 0.006 \pm 0.004$	0.13	4.84
	F_2	$0.555 \pm 0.007 \pm 0.012 \pm 0.010$	0.38	4.20	G_2	$0.026 \pm 0.006 \pm 0.012 \pm 0.010$	-0.01	2.89
	F_3	$-0.252 \pm 0.008 \pm 0.008 \pm 0.013$	0.46	4.29	G_3	$-0.022 \pm 0.025 \pm 0.040 \pm 0.025$	1.04	1.71*
$\Xi_b'^- \rightarrow \Xi_c'^0$	F_1	$0.565 \pm 0.019 \pm 0.023 \pm 0.001$	0.44	4.11	G_1	$-0.197 \pm 0.010 \pm 0.006 \pm 0.004$	0.13	4.84
	F_2	$0.555 \pm 0.007 \pm 0.012 \pm 0.010$	0.38	4.20	G_2	$0.025 \pm 0.006 \pm 0.012 \pm 0.010$	-0.01	2.89
	F_3	$-0.252 \pm 0.008 \pm 0.008 \pm 0.013$	0.46	4.29	G_3	$-0.021 \pm 0.025 \pm 0.040 \pm 0.025$	1.04	1.71*
$\Omega_b^- \rightarrow \Omega_c^0$	F_1	$0.532 \pm 0.021 \pm 0.026 \pm 0.004$	0.44	3.95	G_1	$-0.184 \pm 0.011 \pm 0.007 \pm 0.006$	0.17	4.60
	F_2	$0.529 \pm 0.010 \pm 0.015 \pm 0.016$	0.37	4.00	G_2	$0.021 \pm 0.007 \pm 0.011 \pm 0.011$	0.11	2.58
	F_3	$-0.245 \pm 0.005 \pm 0.017 \pm 0.019$	0.40	4.00	G_3	$-0.009 \pm 0.026 \pm 0.041 \pm 0.028$	-0.07	0.26

Numerical results of these form factors are given in Table III and our results are generally consistent with the previous work [36,59]. The q^2 dependence of these form factors are also fitted with the pole model in Eqs. (26) and (27) since the validity of the pole model with the vector and axial-vector form factors in LFQM has been verified in many studies [36,60–62].

To analyze the q^2 dependence of the form factors, we also plot the results of the form factors as functions of q^2 in Figs. 1 and 2. Since the main focus is the tensor form factors for two types of processes, $\bar{3} \rightarrow \bar{3}$ and $6 \rightarrow 6$, we use $\Lambda_b \rightarrow \Lambda_c$ and $\Sigma_b^+ \rightarrow \Sigma_c^{++}$ as examples. From Figs. 1 and 2, one can see that the fit results with two different models are broadly consistent with each other. However, the q^2 -dependent form factor f_4 exhibits a large discrepancy with $q^2 \sim (m_{B_b} - m_{B_c})^2$ for both models. In the analysis presented in Ref. [63], the form factor has a pole

structure corresponding to the specific current. In our work, the pole mass m_{pole} should be set to $m_{\text{pole}} = m_{B_c}$, which is consistent with the BCL model in Eq. (25). However, the fit result of f_4 with the pole model is different from our conclusion, especially for the $\Lambda_b \rightarrow \Lambda_c$ process. Therefore, it is likely that the BCL model describes the q^2 dependence of the form factor better. Nonetheless, we will still present the results obtained using the pole model since this model is widely used in the light-front approach analysis [40,64].

B. Phenomenological analysis with scalar leptoquarks

Since the form factors induced by SM and BSM currents have been calculated above, we also give a brief phenomenological analysis that includes the tensor current. Specifically, we investigate the NP effect in the

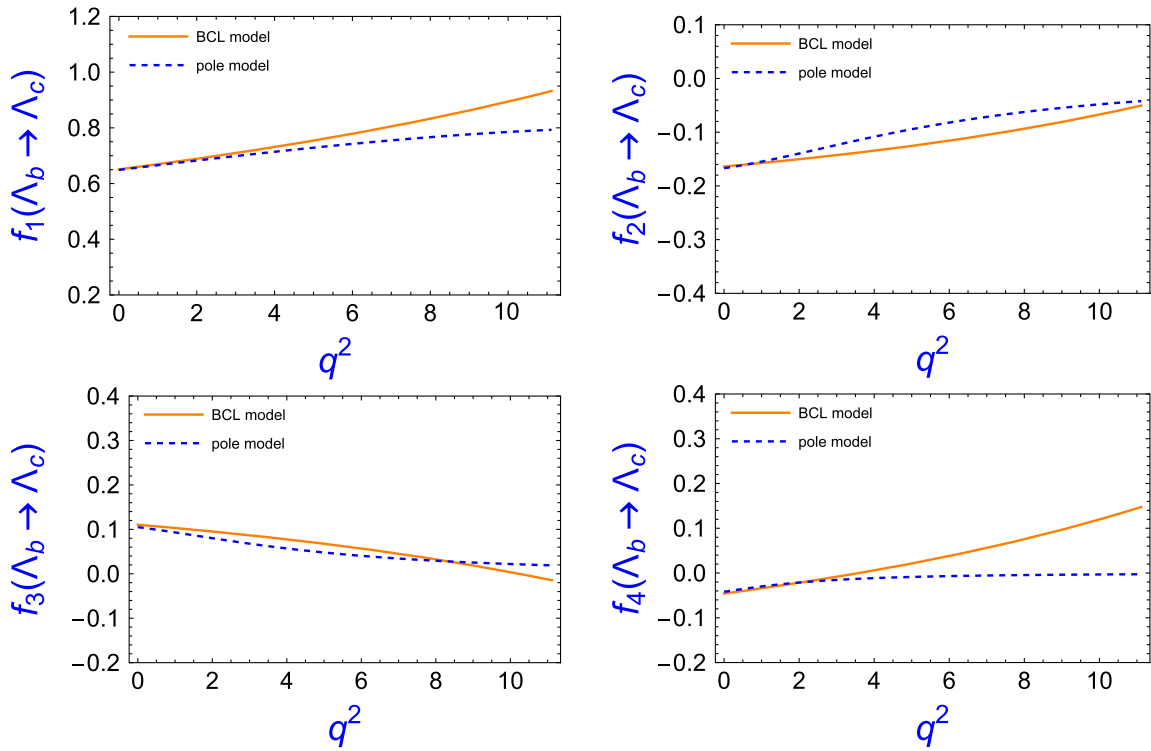


FIG. 1. The q^2 dependence form factors of $\Lambda_b \rightarrow \Lambda_c$ process with BCL model (blue line) and pole model (orange line).

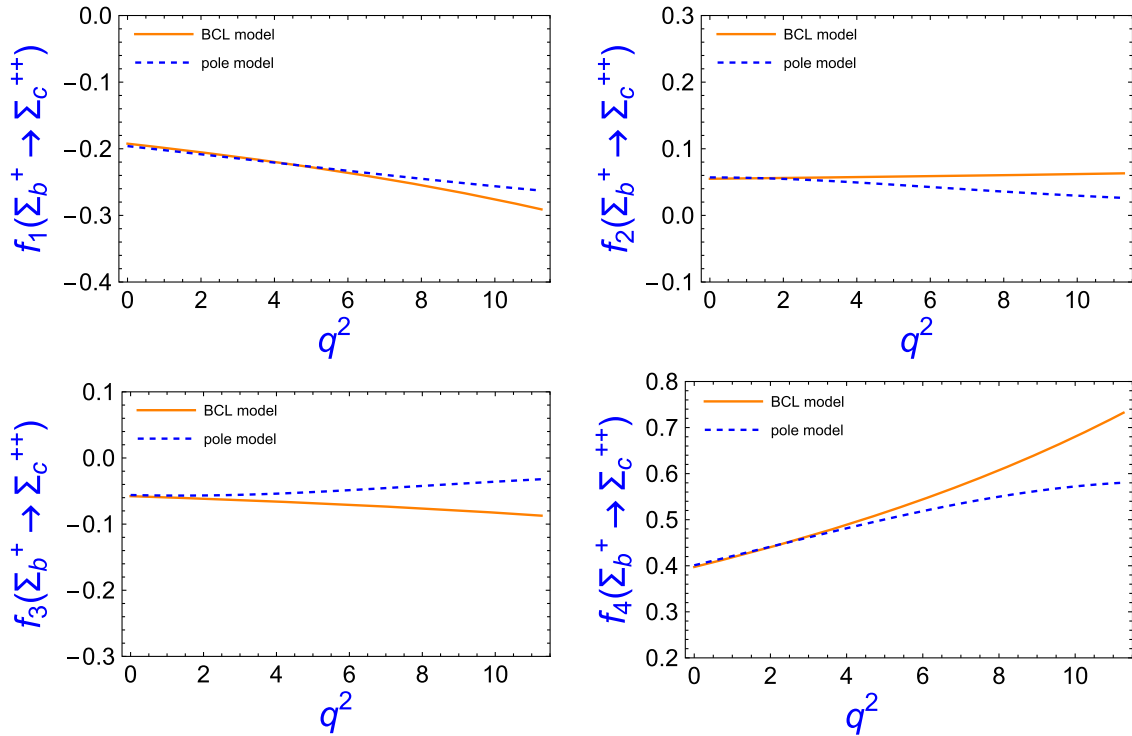


FIG. 2. The q^2 -dependent form factors of $\Sigma_b^+ \rightarrow \Sigma_c^{++}$ process with BCL model (blue line) and pole model (orange line).

scalar leptoquarks model, which has been proposed as a possible scenario to explain the anomaly in $\mathcal{R}(D^{(*)})$ [65]. In our work, the scalar leptoquark $S_1 = (\bar{\mathbf{3}}, \mathbf{1}, 1/3)$: an $SU(2)_L$ singlet scalar is used and the pertinent effective Hamiltonian is given as

$$\begin{aligned} \mathcal{H}_{\text{eff}} &= 2\sqrt{2}G_F V_{cb} [(1 + C_{V_L}^\ell) O_{V_L}^\ell + C_{S_L}^\ell O_{S_L}^\ell + C_T^\ell O_T^\ell], \\ O_{V_L}^\ell &= [\bar{c}\gamma^\mu P_L b][\bar{\ell}\gamma_\mu P_L \nu_\ell], \quad O_{S_L}^\ell = [\bar{c}P_L b][\bar{\ell}P_L \nu_\ell], \\ O_T^\ell &= [\bar{c}\sigma^{\mu\nu} P_L b][\bar{\ell}\sigma_{\mu\nu} P_L \nu_\ell], \end{aligned} \quad (29)$$

where the Wilson coefficient C_i^ℓ vanishes in the SM and reflects the NP contributions. In our work, we consider the NP effect in $b \rightarrow c\tau\nu$ processes. To evaluate the branching ratios $\mathcal{B}(\Lambda_b \rightarrow \Lambda_c \ell \bar{\nu})$ and the ratio $\mathcal{R}(\Lambda_c) = \frac{\mathcal{B}(\Lambda_b \rightarrow \Lambda_c \tau \bar{\nu})}{\mathcal{B}(\Lambda_b \rightarrow \Lambda_c \ell \bar{\nu})}$, baryonic matrix elements are required. The matrix elements with tensor and $(V-A)$ currents are parametrized by the form factors in Eqs. (6) and (28). The $(S-P)$ type matrix element can be expressed by the form factors in a matrix element with $(V-A)$ current by multiplying the q^μ as

$$\begin{aligned} &\langle \mathcal{B}'(P', S') | \bar{c}(1 - \gamma_5)b | \mathcal{B}(P, S) \rangle \\ &= \bar{u}(P', S') \left[F_1(q^2) \frac{m_B - m_{B'}}{m_b - m_c} + F_3(q^2) \frac{q^2}{M_B(m_b - m_c)} \right. \\ &\quad \left. - \left(G_1(q^2) \frac{m_B + m_{B'}}{m_b + m_c} + G_3(q^2) \frac{q^2}{M_B(m_b + m_c)} \right) \gamma_5 \right] \\ &\quad \times u(P, S). \end{aligned} \quad (30)$$

Then the decay width can be expressed as

$$\begin{aligned} \frac{d\Gamma}{dq^2} &= \frac{G_F^2 |V_{CKM}|^2 \sqrt{s_- s_+} (1 - \hat{m}_\ell^2)}{2 \cdot 512\pi^3 M^3} \\ &\quad \times (|C_{S_L}^\ell|^2 L_S + |1 + C_{V_L}^\ell|^2 L_V + |C_T^\ell|^2 L_T \\ &\quad + \mathcal{R}_e(C_{S_L}^{\ell*} (1 + C_{V_L}^\ell)) L_{SV} + \mathcal{R}_e((1 + C_{V_L}^{\ell*}) C_T^\ell) L_{VT}), \end{aligned} \quad (31)$$

where the coefficient L_i is given in the Appendix. For the $\Lambda_b \rightarrow \Lambda_c \ell \nu$, $\ell = e, \mu$ processes, only L_V contributions exist, and the Wilson coefficients C_i^ℓ are zero. As a result, the SM prediction for the branching ratio of $\Lambda_b \rightarrow \Lambda_c \ell \nu$, $\ell = e, \mu$ processes is $\mathcal{B}(\Lambda_b \rightarrow \Lambda_c \ell \nu) = (8.84 \pm 0.85)\%$, which is consistent with the experimental observation $\mathcal{B}(\Lambda_b \rightarrow \Lambda_c \ell \nu) = (6.4_{-1.3}^{+1.4})\%$ listed in the PDG within 2σ . Using the aforementioned branching ratio, the SM prediction for the ratio of branching fractions is $\mathcal{R}(\Lambda_c) = 0.28 \pm 0.05$, which is larger than the experimental result $\mathcal{R}_{\text{exp}}(\Lambda_c) = 0.242 \pm 0.026 \pm 0.040 \pm 0.059$ in Eq. (1).

Using the form factors, the ratio of branching fractions $\mathcal{R}(\Lambda_c)$ can be represented as the function of three NP Wilson coefficients as

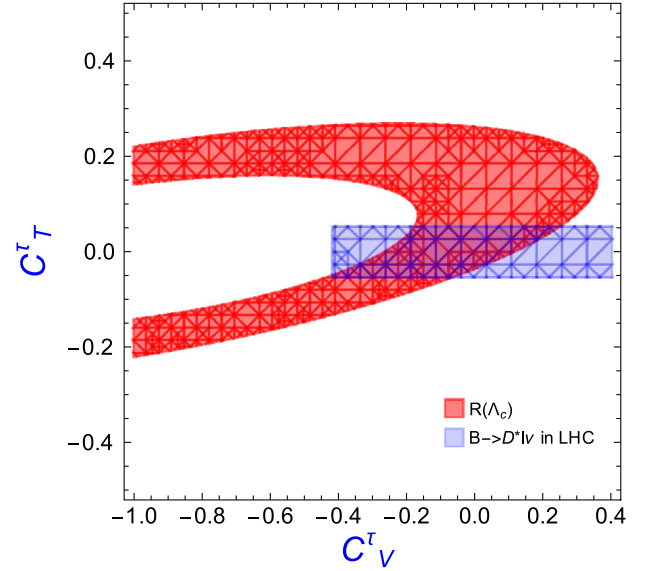


FIG. 3. The constraint on $C_{V_L}^\tau$ and C_T^τ from the $\mathcal{R}_{\text{exp}}(\Lambda_c) = 0.242 \pm 0.026 \pm 0.040 \pm 0.059$ (red) and $B \rightarrow D^* \ell \nu$ data in LHC (blue).

$$\begin{aligned} \mathcal{R}(\Lambda_c) &= M_S |C_{S_L}^\tau|^2 + M_V |1 + C_{V_L}^\tau|^2 + M_T |C_T^\tau|^2 \\ &\quad + M_{SV} \mathcal{R}_e(C_{S_L}^{\tau*} (1 + C_{V_L}^\tau)) \\ &\quad + M_{VT} \mathcal{R}_e((1 + C_{V_L}^{\tau*}) C_T^\tau), \\ M_S &= 0.063 \pm 0.008, \quad M_V = 0.283 \pm 0.027, \\ M_T &= 2.54 \pm 0.66, \quad M_{SV} = 0.071 \pm 0.013, \\ M_{VT} &= -0.88 \pm 0.14. \end{aligned} \quad (32)$$

In the scale $\mu = m_b$, the Wilson coefficients $C_{S_L}^\tau$ and C_T^τ have the relation $C_{S_L}^\tau(\mu) \simeq -7.8 C_T^\tau(\mu)$ [65] by integrating out the $SU(2)_L$ singlet scalar leptoquark. In the assumption that all the NP Wilson coefficients are real, we can give the constraint on the $C_{V_L}^\tau$ and C_T^τ based on the $\mathcal{R}_{\text{exp}}(\Lambda_c) = 0.242 \pm 0.026 \pm 0.040 \pm 0.059$ in Fig. 3. We also note that the Wilson coefficients C_T^τ and $C_{V_L}^\tau$ are constrained by the LHC data in Ref. [66] as $|C_{V_L}^\tau| < 0.42$, $|C_T^\tau| < 0.052$ which are also given in Fig. 3. This figure shows that the NP Hamiltonian in Eq. (29) can explain the \mathcal{R}_{exp} in the region constrained by LHC.

V. SUMMARY

In our work, we presented an exploration of the form factors in the hadronic matrix element with a tensor current. With the help of the LFQM, hadron states can be expressed in terms of relativistic quark-diquark configurations, from which the form factors are extracted. In our calculation, we have calculated the form factors in the $q^2 < 0$ region and accessed their q^2 dependence using both the Bourrely-Caprini-Lellouch parametrization model and the pole

model. The difference between the two models is shown in Figs. 1 and 2 and the results with two different models are generally consistent with each other.

Using the obtained form factors, we give a brief analysis of the scalar leptoquark model $S_1 = (\bar{\mathbf{3}}, \mathbf{1}, 1/3)$ to explain the experiment data $\mathcal{R}_{\text{exp}}(\Lambda_c) = 0.242 \pm 0.026 \pm 0.040 \pm 0.059$. Our results show the NP Hamiltonian in Eq. (29) can explain the \mathcal{R}_{exp} in the region constrained by LHC.

Our work provides the ingredients for further research on the tensor current and its contribution in NP analysis. The phenomenological analysis of new physics contributions made on these form factors can serve as a useful reference for future experimental and theoretical studies.

ACKNOWLEDGMENTS

We thank Dr. Jin Sun for useful discussions and thank Dr. Fei Huang and Mr. Chang Yang for their continued interest. This work is supported in part by the National Natural Science Foundation of China under Grants No. U2032102, No. 12090064, and No. 12125503, by Natural Science Foundation of Shanghai under Grant No. 15DZ2272100, and by China Postdoctoral Science Foundation under Grant No. 2022M72210.

APPENDIX: HELICITY AMPLITUDES

In this section, we collect all helicity amplitudes used in the main text.

$$\begin{aligned}
L_S &= 4(1 - \hat{m}_\ell^2)q^2(|H_{-\frac{1}{2}}^{-\frac{1}{2}}|^2 + |H_{\frac{1}{2}}^{\frac{1}{2}}|^2), \\
L_V &= \frac{4}{3}(1 - \hat{m}_\ell^2)q^2 \left((2 + \hat{m}_\ell^2) \left(|H_{0,-\frac{1}{2}}^{-\frac{1}{2}}|^2 + |H_{1,\frac{1}{2}}^{-\frac{1}{2}}|^2 + |H_{0,\frac{1}{2}}^{\frac{1}{2}}|^2 + |H_{-1,-\frac{1}{2}}^{\frac{1}{2}}|^2 \right) + 3\hat{m}_\ell^2 \left(|H_{t,\frac{1}{2}}^{\frac{1}{2}}|^2 + |H_{t,-\frac{1}{2}}^{-\frac{1}{2}}|^2 \right) \right), \\
L_T &= \frac{8}{3}(1 - \hat{m}_\ell^2)(1 + 2\hat{m}_\ell^2)q^2 \left(|H_{t,0,\frac{1}{2}}^{\frac{1}{2}} + H_{-1,1,\frac{1}{2}}^{\frac{1}{2}}|^2 + |H_{t,0,-\frac{1}{2}}^{-\frac{1}{2}} + H_{-1,1,-\frac{1}{2}}^{-\frac{1}{2}}|^2 + |H_{0,1,\frac{1}{2}}^{-\frac{1}{2}} + H_{3,1,\frac{1}{2}}^{-\frac{1}{2}}|^2 + |H_{-1,0,-\frac{1}{2}}^{\frac{1}{2}} + H_{3,-1,-\frac{1}{2}}^{\frac{1}{2}}|^2 \right), \\
L_{SV} &= 8(1 - \hat{m}_\ell^2)\hat{m}_\ell q^2 \mathcal{R}_e \left(H_{\frac{1}{2}}^{\frac{1}{2}*} H_{t,\frac{1}{2}}^{\frac{1}{2}} + H_{-\frac{1}{2}}^{-\frac{1}{2}*} H_{t,-\frac{1}{2}}^{-\frac{1}{2}} \right), \\
L_{VT} &= 16(1 - \hat{m}_\ell^2)\hat{m}_\ell q^2 \mathcal{R}_e \left(H_{0,\frac{1}{2}}^{\frac{1}{2}*} \left(H_{-1,1,\frac{1}{2}}^{\frac{1}{2}} + H_{t,0,\frac{1}{2}}^{\frac{1}{2}} \right) + H_{-1,-\frac{1}{2}}^{-\frac{1}{2}*} \left(H_{-1,0,-\frac{1}{2}}^{-\frac{1}{2}} + H_{t,-1,-\frac{1}{2}}^{-\frac{1}{2}} \right) + H_{0,-\frac{1}{2}}^{-\frac{1}{2}*} \left(H_{-1,1,-\frac{1}{2}}^{-\frac{1}{2}} + H_{t,0,-\frac{1}{2}}^{-\frac{1}{2}} \right) \right. \\
&\quad \left. + H_{1,\frac{1}{2}}^{\frac{1}{2}*} \left(H_{0,1,\frac{1}{2}}^{\frac{1}{2}} + H_{t,1,\frac{1}{2}}^{\frac{1}{2}} \right) \right).
\end{aligned}$$

where

$$\begin{aligned}
H_{S'}^S &= HS_{S'}^S - HP_{S'}^S = \langle \mathcal{B}'(P', S') | \bar{c}(1 - \gamma_5)b | \mathcal{B}(P, S) \rangle, \\
H_{S_w, S'}^S &= HV_{S_w, S'}^S - HA_{S_w, S'}^S = \langle \mathcal{B}'(P', S') | \bar{c}\gamma^\mu(1 - \gamma_5)b | \mathcal{B}(P, S) \rangle \epsilon_\mu^*(S_w), \\
H_{S_{w1}, S_{w2}, S'}^S &= HT_{S_{w1}, S_{w2}, S'}^S - HTS_{S_{w1}, S_{w2}, S'}^S = \langle \mathcal{B}'(P', S') | \bar{c}i\sigma^{\mu\nu}(1 - \gamma_5)b | \mathcal{B}(P, S) \rangle \epsilon_\mu^*(S_{w1})\epsilon_\nu^*(S_{w2}).
\end{aligned}$$

The $HS_{S'}^S$, $HV_{S_w, S'}^S$, $HT_{S_{w1}, S_{w2}, S'}^S$ are helicity amplitudes which can be expressed by form factors defined in Eqs. (6), (28), and (30). Based on the same convention, the helicity amplitude with $(S - P)$ and $(V - A)$ can be expressed as

$$\begin{aligned}
HS_{\frac{1}{2}}^{\frac{1}{2}} &= \sqrt{Q_+} \left(F_1 \frac{M - M'}{m_b - m_c} + F_3 \frac{q^2}{(m_b - m_c)M} \right) & HP_{\frac{1}{2}}^{\frac{1}{2}} &= \sqrt{Q_-} \left(-G_1 \frac{M + M'}{m_b + m_c} - G_3 \frac{q^2}{(m_b + m_c)M} \right), \\
HV_{0,\frac{1}{2}}^{\frac{1}{2}} &= \sqrt{\frac{Q_-}{q^2}} \left(F_1(M + M') - F_2 \frac{q^2}{M} \right), & HA_{0,\frac{1}{2}}^{\frac{1}{2}} &= \sqrt{\frac{Q_+}{q^2}} \left(G_1(M - M') + G_2 \frac{q^2}{M} \right), \\
HV_{t,\frac{1}{2}}^{\frac{1}{2}} &= \sqrt{\frac{Q_+}{q^2}} \left(F_1(M - M') + F_3 \frac{q^2}{M} \right), & HA_{t,\frac{1}{2}}^{\frac{1}{2}} &= \sqrt{\frac{Q_-}{q^2}} \left(G_1(M + M') - G_3 \frac{q^2}{M} \right), \\
HV_{1,\frac{1}{2}}^{-\frac{1}{2}} &= \sqrt{2Q_-} \left(F_1 - F_2 \frac{M + M'}{M} \right), & HA_{1,\frac{1}{2}}^{-\frac{1}{2}} &= \sqrt{2Q_+} \left(G_1 + G_2 \frac{M - M'}{M} \right), \\
HS_{-\frac{1}{2}}^{-\frac{1}{2}} &= HS_{\frac{1}{2}}^{\frac{1}{2}}, & HP_{-\frac{1}{2}}^{-\frac{1}{2}} &= -HP_{\frac{1}{2}}^{\frac{1}{2}}, & HV_{-S_w, -S'}^{-S} &= HV_{S_w, S'}^S, & HA_{-S_w, -S'}^{-S} &= -HA_{S_w, S'}^S.
\end{aligned}$$

The helicity amplitudes with tensor current are

$$\begin{aligned}
HT_{t,0,\frac{1}{2}}^{\frac{1}{2}} &= \sqrt{Q_-} \left(f_1 - f_2 + f_3 + f_4 \frac{Q_+}{2MM'} \right), \quad HT_{t,0,\frac{1}{2}}^{5\frac{1}{2}} = -\sqrt{Q_+} f_1, \quad HT_{1,-1,\frac{1}{2}}^{\frac{1}{2}} = -f_1 \sqrt{Q_+}, \quad HT_{1,-1,\frac{1}{2}}^{5\frac{1}{2}} = -HT_{t,0,\frac{1}{2}}^{\frac{1}{2}} \\
HT_{1,t,\frac{1}{2}}^{\frac{1}{2}} &= \sqrt{\frac{2Q_-}{q^2}} \left(-f_1(M+M') + f_2 \frac{M^2 - M'^2 + q^2}{2M} + f_3 \frac{M^2 - M'^2 - q^2}{2M'} \right), \\
HT_{1,t,\frac{1}{2}}^{5\frac{1}{2}} &= -\sqrt{\frac{2Q_+}{q^2}} \left(-f_1(M-M') + f_2 \frac{Q_-}{2M} + f_3 \frac{Q_-}{2M'} \right) \quad HT_{1,0,\frac{1}{2}}^{-\frac{1}{2}} = -HT_{1,t,\frac{1}{2}}^{5\frac{1}{2}}, \quad HT_{1,0,\frac{1}{2}}^{5-\frac{1}{2}} = -HT_{1,t,\frac{1}{2}}^{-\frac{1}{2}},
\end{aligned}$$

$$HT_{-S_{w1},-S_{w2},-S'}^{-S} = HT_{S_{w1},S_{w2},S'}^S, \quad HT_{-S_{w1},-S_{w2},-S'}^{5-S} = -HT_{S_{w1},S_{w2},S'}^S, \quad H_{S_{w2},S_{w1},S'}^S = -H_{S_{w1},S_{w2},S'}^S,$$

where $Q_{\pm} = (M \pm M')^2 - q^2$. The other helicity amplitudes are zero.

-
- [1] J. P. Lees *et al.* (BABAR Collaboration), *Phys. Rev. Lett.* **109**, 101802 (2012).
- [2] J. P. Lees *et al.* (BABAR Collaboration), *Phys. Rev. D* **88**, 072012 (2013).
- [3] M. Huschle *et al.* (Belle Collaboration), *Phys. Rev. D* **92**, 072014 (2015).
- [4] Y. Sato *et al.* (Belle Collaboration), *Phys. Rev. D* **94**, 072007 (2016).
- [5] S. Hirose *et al.* (Belle Collaboration), *Phys. Rev. Lett.* **118**, 211801 (2017).
- [6] S. Hirose *et al.* (Belle Collaboration), *Phys. Rev. D* **97**, 012004 (2018).
- [7] G. Caria *et al.* (Belle Collaboration), *Phys. Rev. Lett.* **124**, 161803 (2020).
- [8] LHCb Collaboration, [arXiv:2302.02886](https://arxiv.org/abs/2302.02886).
- [9] R. Aaij *et al.* (LHCb Collaboration), [arXiv:2305.01463](https://arxiv.org/abs/2305.01463).
- [10] R. Aaij *et al.* (LHCb Collaboration), *Phys. Rev. Lett.* **120**, 121801 (2018).
- [11] R. Aaij *et al.* (LHCb Collaboration), *Phys. Rev. Lett.* **128**, 191803 (2022).
- [12] Y. S. Amhis *et al.* (Heavy Flavor Averaging Group and HFLAV Collaboration), *Phys. Rev. D* **107**, 052008 (2023).
- [13] J. Harrison, C. T. H. Davies, and A. Lytle (LATTICE-HPQCD Collaboration), *Phys. Rev. Lett.* **125**, 222003 (2020).
- [14] F. U. Bernlochner, Z. Ligeti, D. J. Robinson, and W. L. Sutcliffe, *Phys. Rev. D* **99**, 055008 (2019).
- [15] S. Iguro, T. Kitahara, and R. Watanabe, [arXiv:2210.10751](https://arxiv.org/abs/2210.10751).
- [16] Y. Li and C. D. Lü, *Sci. Bull.* **63**, 267 (2018).
- [17] S. Shivashankara, W. Wu, and A. Datta, *Phys. Rev. D* **91**, 115003 (2015).
- [18] X. Q. Li, Y. D. Yang, and X. Zhang, *J. High Energy Phys.* **02** (2017) 068.
- [19] X. H. Hu and Z. X. Zhao, *Chin. Phys. C* **43**, 093104 (2019).
- [20] Z. X. Zhao, R. H. Li, Y. L. Shen, Y. J. Shi, and Y. S. Yang, *Eur. Phys. J. C* **80**, 1181 (2020).
- [21] D. Shen, H. Ren, F. Wu, and R. Zhu, *Int. J. Mod. Phys. A* **36**, 2150135 (2021).
- [22] W. Tao, Z. J. Xiao, and R. Zhu, *Phys. Rev. D* **105**, 114026 (2022).
- [23] P. Biancofiore, P. Colangelo, and F. De Fazio, *Phys. Rev. D* **87**, 074010 (2013).
- [24] R. Y. Tang, Z. R. Huang, C. D. Lü, and R. Zhu, *J. Phys. G* **49**, 115003 (2022).
- [25] M. L. Du, N. Penalva, E. Hernández, and J. Nieves, *Phys. Rev. D* **106**, 055039 (2022).
- [26] M. Fedele, M. Blanke, A. Crivellin, S. Iguro, T. Kitahara, U. Nierste, and R. Watanabe, *Phys. Rev. D* **107**, 055005 (2023).
- [27] W. Jaus, *Phys. Rev. D* **41**, 3394 (1990).
- [28] W. Jaus, *Phys. Rev. D* **44**, 2851 (1991).
- [29] H. Y. Cheng, C. Y. Cheung, and C. W. Hwang, *Phys. Rev. D* **55**, 1559 (1997).
- [30] W. Jaus, *Phys. Rev. D* **60**, 054026 (1999).
- [31] H. Y. Cheng, C. K. Chua, and C. W. Hwang, *Phys. Rev. D* **69**, 074025 (2004).
- [32] M. D. Scadron, G. Rupp, F. Kleefeld, and E. van Beveren, *Phys. Rev. D* **69**, 014010 (2004); **69**, 059901(E) (2004).
- [33] Z. P. Xing and Z. X. Zhao, *Phys. Rev. D* **98**, 056002 (2018).
- [34] Z. X. Zhao, *Eur. Phys. J. C* **78**, 756 (2018).
- [35] Z. X. Zhao, [arXiv:2204.00759](https://arxiv.org/abs/2204.00759).
- [36] H. W. Ke, N. Hao, and X. Q. Li, *Eur. Phys. J. C* **79**, 540 (2019).
- [37] F. Lu, H. W. Ke, X. H. Liu, and Y. L. Shi, *Eur. Phys. J. C* **83**, 412 (2023).
- [38] Z. R. Huang, Y. Li, C. D. Lu, M. A. Paracha, and C. Wang, *Phys. Rev. D* **98**, 095018 (2018).
- [39] J. Harrison and C. T. H. Davies, [arXiv:2304.03137](https://arxiv.org/abs/2304.03137).
- [40] X. H. Hu, R. H. Li, and Z. P. Xing, *Eur. Phys. J. C* **80**, 320 (2020).
- [41] Y. S. Li and X. Liu, *Phys. Rev. D* **107**, 033005 (2023).
- [42] Z. X. Zhao, F. W. Zhang, X. H. Hu, and Y. J. Shi, *Phys. Rev. D* **107**, 116025 (2023).
- [43] W. Wang and Z. P. Xing, *Phys. Lett. B* **834**, 137402 (2022).
- [44] T. M. Aliev, A. Ozpineci, and V. Zamiralov, *Phys. Rev. D* **83**, 016008 (2011).
- [45] Y. Matsui, *Nucl. Phys.* **A1008**, 122139 (2021).

- [46] X. G. He, F. Huang, W. Wang, and Z. P. Xing, *Phys. Lett. B* **823**, 136765 (2021).
- [47] C. Q. Geng, X. N. Jin, and C. W. Liu, *Phys. Lett. B* **838**, 137736 (2023).
- [48] H. W. Ke and X. Q. Li, *Phys. Rev. D* **105**, 096011 (2022).
- [49] Z. P. Xing and Y. j. Shi, *Phys. Rev. D* **107**, 074024 (2023).
- [50] H. Liu, L. Liu, P. Sun, W. Sun, J. X. Tan, W. Wang, Y. B. Yang, and Q. A. Zhang, *Phys. Lett. B* **841**, 137941 (2023).
- [51] Z. S. Brown, W. Detmold, S. Meinel, and K. Orginos, *Phys. Rev. D* **90**, 094507 (2014).
- [52] G. Li, F. l. Shao, and W. Wang, *Phys. Rev. D* **82**, 094031 (2010).
- [53] R. C. Verma, *J. Phys. G* **39**, 025005 (2012).
- [54] Y. J. Shi, W. Wang, and Z. X. Zhao, *Eur. Phys. J. C* **76**, 555 (2016).
- [55] C. G. Boyd, B. Grinstein, and R. F. Lebed, *Phys. Rev. D* **56**, 6895 (1997).
- [56] I. Caprini, L. Lellouch, and M. Neubert, *Nucl. Phys.* **B530**, 153 (1998).
- [57] C. Bourrely, I. Caprini, and L. Lellouch, *Phys. Rev. D* **79**, 013008 (2009); **82**, 099902(E) (2010).
- [58] A. Bharucha, T. Feldmann, and M. Wick, *J. High Energy Phys.* **09** (2010) 090.
- [59] Y. Miao, H. Deng, K. S. Huang, J. Gao, and Y. L. Shen, *Chin. Phys. C* **46**, 113107 (2022).
- [60] H. W. Ke, X. Q. Li, and Z. T. Wei, *Phys. Rev. D* **77**, 014020 (2008).
- [61] H. W. Ke, X. H. Yuan, X. Q. Li, Z. T. Wei, and Y. X. Zhang, *Phys. Rev. D* **86**, 114005 (2012).
- [62] H. W. Ke, N. Hao, and X. Q. Li, *J. Phys. G* **46**, 115003 (2019).
- [63] H. Liu, Z. P. Xing, and C. Yang, *Eur. Phys. J. C* **83**, 123 (2023).
- [64] Q. Chang, X. L. Wang, and L. T. Wang, *Chin. Phys. C* **44**, 083105 (2020).
- [65] Y. Sakaki, M. Tanaka, A. Tayduganov, and R. Watanabe, *Phys. Rev. D* **88**, 094012 (2013).
- [66] S. Iguro, M. Takeuchi, and R. Watanabe, *Eur. Phys. J. C* **81**, 406 (2021).